MOF Phase Transitions

DOI: 10.1002/anie.201411005

A 36-Fold Multiple Unit Cell and Switchable Anisotropic Dielectric Responses in an Ammonium Magnesium Formate Framework**

Ran Shang, Zhe-Ming Wang, and Song Gao**

Abstract: *An ammonium Mg formate framework, prepared by using di-protonated 1,3-propanediamine (pnH_2^{2+}), has a rare three-dimensional binodal $(4^{12}\cdot6^3)(4^9\cdot6^6)_3$ Mg-formate framework with elongated cavities accommodating $pnH_2^{2+}\cdots H_2O\cdots pnH_2^{2+}$ assemblies. It displays a para-electric to antiferroelectric phase transition at 275 K, with a 36-fold multiple unit cell from the high-temperature cell of 1703 Å^3 to the low-temperature one of 60 980 Å^3. The change results from the disorder–order transition of the pnH_2^{2+} cations and H_2O molecules. The motions of these components freeze in a stepwise fashion on going from the high-temperature disorder state to the low-temperature ordered state, triggering the switch from high to low dielectric constants, and the spatial limitation of such motions contributes the strong dielectric anisotropy.*

Metal–organic frameworks (MOFs) have been exploited for the abundance of their phase transitions and related properties, which can be comparable to those of conventional materials, such as oxides.[1] MOFs are especially promising for generating dielectric/ferroelectric/antiferroelectric (DE/FE/AFE) properties. This promise arises because the labile hydrogen-bonding systems and/or mobile polar components required for these properties can be incorporated, and the change in their dynamics and/or status can be tailored, if suitable building blocks are chosen and properly organized into MOFs.[2–4] Furthermore, MOF-multiferroics have emerged through the synergy/coexistence of magnetic and electric orderings.[5] In this context, ammonium metal formate frameworks (AMFFs)[6] have been shown to exhibit abundant and interesting DE/FE/AFE, magnetic and mechanical properties, structural phase transitions, and possible multiferroics, because they possess the required hydrogen bonding, magnetic couplings, and disorder–order alterations of ammonium.[7–13] The freezing of the vibration, flipping, twisting, and rotation of ammonium molecules could result in framework distortion thus lower lattice symmetries, and/or a multiple unit cell, that is, the high-temperature (HT) small unit cell is multiple below the critical or transition temperature (T_C) due to the antipolarization in low-temperature (LT) region. These are similar to traditional oxides, such as $BaTiO_3$ (showing no multiple unit cell) and $PbZrO_3$ (showing multiple unit cell).[14] Up to nine-fold multiple unit cells have been observed in AMFFs, accompanied by the interesting DE/FE/AFE behaviors.[9–12] More complicated disorder–order transitions and patterns of multiple unit cells will be expected if polyammoniums are used, because of the increased number of ordered states possible for the flexible components.[11a–c,13] We report herein a Mg AMFF incorporating di-protonated 1,3-propanediamine (pnH_2^{2+}) and water, formulated as $[(pnH_2^{2+})_2(H_2O)][Mg(HCOO)_3]_4$ (**1**). The material has a rare three-dimensional (3D) binodal $(4^{12}\cdot6^3)(4^9\cdot6^6)_3$[15] Mg-formate framework with elongated cavities, each accommodating one $pnH_2^{2+}\cdots H_2O\cdots pnH_2^{2+}$ assembly. It showed a phase transition at the critical temperature (T_C) of 275 K, with an unprecedented 36-fold multiple unit cell from 1703 Å^3 of the HT lattice to 60 980 Å^3 of the LT lattice, and switchable, anisotropic dielectric responses.

The hexagonal plate crystals of **1** were prepared by the reaction of 1,3-propanediamine, formic acid, and $Mg(ClO_4)_2\cdot6H_2O$ in methanol (see Experimental Details and Figure S1 in Supporting Information). The phase purity was confirmed by powder X-ray diffraction (Figure S2), and the material was thermally stable up to 100 °C (Figure S3a). The differential scanning calorimetry (DSC, Figure S3b) revealed a reversible phase transition by the exothermic/endothermic peaks at 273/281 K on cooling/heating, with LT thermal dispersion.[9–11] The ΔH and ΔS were 3.1 kJ mol^{-1} and 11.2 J mol^{-1} K^{-1}, respectively, and the ratio of the state numbers in different phases, $N = 3.9$, by using $\Delta S = R\ln(N)$. The variable temperature (VT) oscillation images (OSCIs, Figure 1, Figures S4 and S5) provided further information.[10,11b,c,13a] On LT OSCIs, many weak spots appeared among the bright spots of the HT reciprocal lattice, indicating a large multiple unit cell. The relationship between the HT and LT reciprocal cells led to $a^{LT} \approx 2(a^{HT} - b^{HT})$, $b^{LT} \approx 2(a^{HT} + 2b^{HT})$, $c^{LT} \approx 3c^{HT}$ and $V^{LT} \approx 36V^{HT}$, and the LT cell is *R*-centered. The 36-fold multiple unit cell is amazing because to our knowledge such a large multiple unit cell has not been reported for any MOF or AMFF.[2–6] It is much larger than the 8-fold multiple unit cell in the AFE $PbZrO_3$,[14] and the 9-fold multiple unit cell in $[(CH_3)_2NH_2][Fe^{III}Fe^{II}(HCOO)_6]$.[12]

The structures at 93, 180, 230, 270, 290, and 320 K were determined (Tables S1 and S2). At 290 K, the crystal belongs to the space group $P\bar{3}1c$, with $a = 8.2923$, $c = 28.5915$ Å, and $V = 1702.6$ Å^3. It has a binodal 3D Mg-formate framework with octahedral $(4^{12}\cdot6^3)$ nodes and trigonal prismatic $(4^9\cdot6^6)$ nodes in a ratio of 1:3, connected by *anti–anti* formate bridges (Figure 2 a,b). The framework thus has a $(4^{12}\cdot6^3)(4^9\cdot6^6)_3$ top-

[*] R. Shang, Prof. Z.-M. Wang, Prof. S. Gao
Beijing National Laboratory for Molecular Sciences, State Key Laboratory of Rare Earth Materials Chemistry and Applications, College of Chemistry and Molecular Engineering, Peking University
Beijing 100871 (China)
E-mail: zmw@pku.edu.cn
gaosong@pku.edu.cn

[**] This work was supported by the NSFC (Grants 21171010, 21290170, 21290171, and 21321001), the National Basic Research Program of China (Grant 2013CB933401).

Supporting information for this article is available on the WWW under http://dx.doi.org/10.1002/anie.201411005.

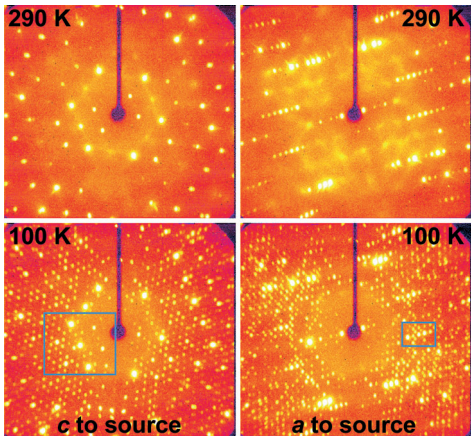

Figure 1. The OSCIs at 290 and 100 K for a crystal of **1**, showing a many-fold multiple unit cell. The parts inside the boxes were used in Figure S5, to show the relationship between the LT and HT reciprocal lattices, see text for details.

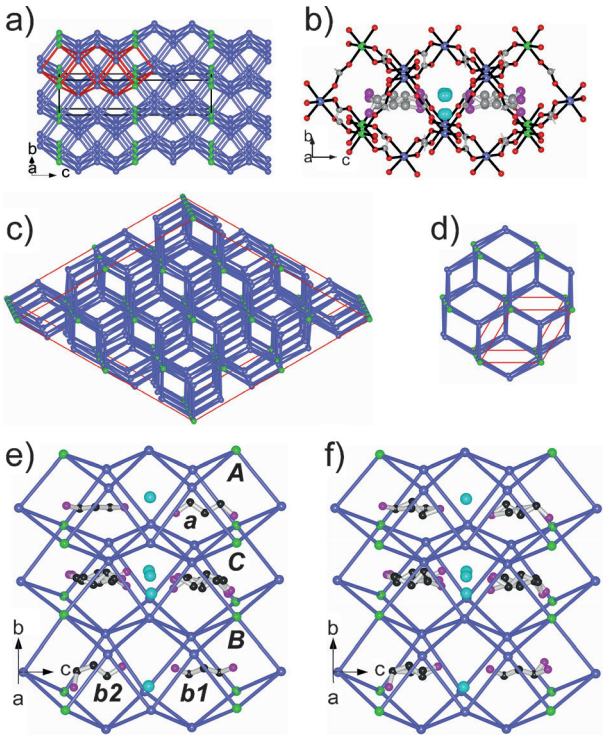

Figure 2. The structures of **1**. a) The topological view of the Mg-formate framework at 290 K, spheres: Mg atoms, sticks: the *anti–anti* HCOO bridges, one cavity is highlighted in red. b) The side view of one cavity with the $pnH_2^{2+}\cdots H_2O\cdots pnH_2^{2+}$ assembly, at 290 K. Topological views of the framework at c) 93 K and d) 290 K, viewed along the *c*-axis, with the unit cells in red boxes. The three neighboring cavities *A*,*B*,*C* at e) 93 K and f) 270 K, showing the stepwise nature the order–disorder transition of the $pnH_2^{2+}\cdots H_2O\cdots pnH_2^{2+}$ part. Color scheme: green for ($4^{12}\cdot6^3$) Mg nodes; violet blue for ($4^9\cdot6^6$) Mg nodes; red for O of HCOO, cyan for O of H_2O; gray/dark gray for C; purple for N; white for H.

ology.[15] It is rare for MOFs and/or AMFFs,[1–6] and one known example is $[tptaH_4][Co(HCOO)_3]_4$ ($tptaH_4^{4+} = H_3N\text{-}(CH_2)_3NH_2(CH_2)_3NH_2(CH_2)_3NH_3$).[6,11a] The framework has long cavities, each accommodating one $pnH_2^{2+}\cdots H_2O\cdots pnH_2^{2+}$ assembly that is similar to $tptaH_4^{4+}$ in length and hydrogen bonding. Both pnH_2^{2+} and the water molecule are disordered in six symmetry-related sites, revealing their rotation or twist motions around the long axis of the cavity, parallel to the *c* axis. The Mg–O distances are 2.063–2.096 Å, the Mg···Mg distances 5.957 to 5.991 Å through formato bridge, and N/O···O distances 2.88–3.30 Å through hydrogen bonds.

Below T_C, the LT lattice becomes $R\bar{3}c$, and has an unit cell approximately 36-times the volume of the HT cell (Figure 2c,d), with $a = 28.5247$, $c = 86.5390$ Å, and $V = 60\,980$ Å^3 at 270 K. The a^{LT} is parallel to a^{*HT}, and the c^{LT} parallel to c^{HT}. The relationship between LT and HT cells is as previously revealed by the study on VT OSCIs. The even-fold multiple unit cell and the alternation in space group indicate a paraelectric (PE) to AFE phase transition.[12,14] The temperature evolutions of the cell parameters and the observations percentage in diffraction intensities (Figure S6a) under the LT lattice setting show abrupt changes around 270 K, evidencing the phase transition. This structural phase transition is caused by the disorder–order alternation of $pnH_2^{2+}\cdots H_2O\cdots pnH_2^{2+}$ parts and the related framework regulation, much more complicated than those in the other AMFFs.[6b,8–13] The slightly distorted LT framework includes three unique, neighboring cavities, labeled *A*, *B*, and *C* (Figure 2e). At 93 K, in *A* and *B* the pnH_2^{2+}–water parts are ordered. In *A* the unique pnH_2^{2+} (labeled *a*) is extended, but in *B* one (labeled *b1*) is extended, the other (labeled *b2*) partially gauche. In *C* both pnH_2^{2+} and water have two major orientations (occupancies 0.46, one pnH_2^{2+} extended and the other partially gauche) and one minor (occupancy of 0.08, pnH_2^{2+} partially extended), indicating the disorder of the part in *C*, probably static, at 93 K. On warming, the major orientations showed decreased occupancies so the minor orientations increased (Figure S6b). Above 200 K, the middle CH_2–CH_2–CH_2 of *b2* and one NH_3 end of *b1* in *B* started to flip, and on further warming, the flipping motion of the middle CH_2–CH_2–CH_2 of *a* in *A* started (Figure 2f). The occupancies decrease for the major orientations of pnH_2^{2+} (and water in *C*) on warming implies the gradually enhancement of the flipping motions, which finally leads to the phase transition, and the three cavities become equivalent (Figure 2b). The stepwise freezing of the flipping motions of pnH_2^{2+} and water is unique,[6b,11] indicating a complicated disorder–order transition for the ammonium and water arising from the flexible character of the $pnH_2^{2+}\cdots H_2O\cdots pnH_2^{2+}$ assembly. It also contributes to the LT thermal dispersion of DSC peaks.[9–11] Counting the site-numbers of the particles of the $pnH_2^{2+}\cdots H_2O\cdots pnH_2^{2+}$ assemblies in three cavities, 36 at 290 K and 18 at 93 K, the *N* value is 2, significantly smaller than 3.9 by DSC. This should be due to the possibility that there are more possible conformations of pnH_2^{2+} in HT phase than the extended one modeled by the structural analysis. In the lattice, the flipping motions of pnH_2^{2+} and water and the enhancement, limited in the *ab* plane, leads to an expansion (+0.3%) in the *a* direction but a contraction (−0.2%) in the *c* direction, indicating the ammonium/water–framework coupled thermal expansion behavior.[4,11] The molecular and hydrogen-bonding geome-

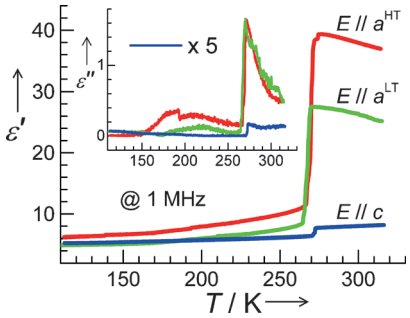

Figure 3. ε' vs T and ε'' vs T (inset) traces for crystals of **1**, with the applied E parallel to a^{HT}, a^{LT}, and c directions, all at 1 MHz.

tries for LT structures show more diversity (Table S2), owing to the structural distortion at LT.

The temperature-dependent complex dielectric permittivities (ε' and ε'') were investigated for the crystals (Figure 3). At 1 MHz, the ε' values at 315 K are 37.0, 27.6,and 8.2 for a^{HT}, a^{LT} and c directions, respectively. When cooling to around 275 K, the ε' traces slightly rise for a^{HT} and a^{LT}, but for c it goes down slightly. Then they drop quickly, with the steep falls around 270 K. The ε' values after the steep falls are 11.6 at 267 K (a^{HT}), 8.5 at 264 K (a^{LT}), and 6.4 at 270 K (c). Below 250 K they decrease slowly, to 6.2 at 112 K (a^{HT}), 4.9 at 110 K (a^{LT}), and 5.3 at 113 K (c). The ε'' vs T traces first exhibit peaks around 270 K, then quickly fall, and below 260 K broad peaks are observed for a^{HT} and a^{LT}, but not for c. The ε'' responses decrease further to small and featureless values below 200 K. For lower frequencies, the $\varepsilon'/\varepsilon''$ vs T traces show the same features (data are not given).

The material features high ε' values at HT but low ε' values at LT, switched by the PE–AFE phase transition at $T_C = 275$ K, and strong anisotropy in the dielectric responses, which are high in the ab plane but low in the c direction. At HT, the pnH_2^{2+} cations and H_2O molecules rotate or twist between the preferred sites in the cavity. Such motions induce dipoles or polarizations and their fluctuations, thus contribute the high ε' but low ε'' values.[14,16] The strong dielectric anisotropy is due to the fact that the motions of pnH_2^{2+} and H_2O are around the c axis or mainly limited in the ab plane.[3a,b] On cooling, the contraction of the lattice and the increased hydrogen-bonding interactions will slow or damp such motions, therefore the ε'' increases.[9,11] After the phase transition, the rotation motions of pnH_2^{2+} and H_2O freeze, but the pnH_2^{2+} cations and some H_2O molecules still flip. Since these flipping motions incorporate a lower number of polar NH_3 ends of pnH_2^{2+} and H_2O molecules and have different dynamics compared to the rotation or twist motions involving all the NH_3 groups and H_2O molecules in the HT phase, the dielectric responses thus significantly drop. On further cooling, such flipping motions gradual freeze, in a stepwise manner, leading to a further slow ε' decrease and broad low ε'' peaks.

In conclusion, the use of pnH_2^{2+} directed a rare 3D binodal $(4^{12}\cdot6^3)(4^9\cdot6^6)_3$ Mg-formate framework with long cavities for accommodating $pnH_2^{2+}\cdots H_2O\cdots pnH_2^{2+}$ assemblies. The material underwent a para-electric–antiferroelectric phase transition at 275 K, and showed a surprising 36-fold multiple unit cell, from a small high-temperature-phase cell of approximately 1700 Å^3 to a large low-temperature-phase cell of approximately 61 000 Å^3. The phase transition was triggered by the disorder–order transition of $pnH_2^{2+}\cdots H_2O\cdots pnH_2^{2+}$ parts, from the sixfold disordered state of pnH_2^{2+} and H_2O in the high-temperature phase to the stepwise freezing of their motion in low-temperature phase. The switchable dielectric behaviors from the high-temperature high ε' value state to the low-temperature low ε' value one, and the significant dielectric anisotropy were rationalized by the variable temperature structural study. This work reveals the abundance of phase transitions and relevant dielectric/ferroelectric/antiferroelectric properties of AMFFs. Further studies will include 1) various flexible polyammoniums could be introduced and a wide spectrum of dielectric/ferroelectric/antiferroelectric properties, phase transitions, and ammonium disorder–order alternation patterns will be expected; 2) magnetic metal ions could be incorporated thus new AMFF-based multiferroics could be created. These researches will certainly enhance our understanding of the multitude of properties and the subtle synergy of the coexisting properties in MOFs.

Received: November 13, 2014
Published online: January 13, 2015

Keywords: ammonium metal formate · dielectricity · metal–organic frameworks · multiple unit cell · phase transition

[1] a) I. E. Collings, A. B. Cairns, A. L. Thompson, J. E. Parker, C. C. Tang, M. G. Tucker, J. Catafesta, C. Levelut, J. Haines, V. Dmitriev, P. Pattison, A. L. Goodwin, *J. Am. Chem. Soc.* **2013**, *135*, 7610–7620; b) T. D. Bennett, J. C. Tan, S. A. Moggach, R. Galvelis, C. Mellot-Draznieks, B. A. Reisner, A. Thirumurugan, D. R. Allan, A. K. Cheetham, *Chem. Eur. J.* **2010**, *16*, 10684–10690; c) S. A. Moggach, T. D. Bennett, A. K. Cheetham, *Angew. Chem. Int. Ed.* **2009**, *48*, 7087–7089; *Angew. Chem.* **2009**, *121*, 7221–7223; d) E. C. Spencer, R. J. Angel, N. L. Ross, B. E. Hanson, J. A. K. Howard, *J. Am. Chem. Soc.* **2009**, *131*, 4022–4026; e) T. D. Bennett, A. L. Goodwin, M. T. Dove, D. A. Keen, M. G. Tucker, E. R. Barney, A. K. Soper, E. G. Bithell, J.-C. Tan, A. K. Cheetham, *Phys. Rev. Lett.* **2010**, *104*, 115503.

[2] W. Zhang, R.-G. Xiong, *Chem. Rev.* **2012**, *112*, 1163–1195.

[3] a) W. Zhang, Y. Cai, R. G. Xiong, H. Yoshikawa, K. Awaga, *Angew. Chem. Int. Ed.* **2010**, *49*, 6608–6610; *Angew. Chem.* **2010**, *122*, 6758–6760; b) W. Zhang, H.-Y. Ye, R. Graf, H. W. Spiess, Y.-F. Yao, R.-Q. Zhu, R.-G. Xiong, *J. Am. Chem. Soc.* **2013**, *135*, 5230–5233; c) Z.-Y. Du, T.-T. Xu, B. Huang, Y.-J. Su, W. Xue, C.-T. He, W.-X. Zhang, X.-M. Chen, *Angew. Chem. Int. Ed.* **2014**, DOI: 10.1002/anie.201408491; *Angew. Chem.* **2014**, DOI: 10.1002/ange.201408491; d) S. Devautour-Vinot, G. Maurin, C. Serre, P. Horcajada, D. P. da Cunha, V. Guillerm, E. de Souza Costa, F. Taulelle, C. Martineau, *Chem. Mater.* **2012**, *24*, 2168–2177; e) P. Sippel, D. Denysenko, A. Loidl, P. Lunkenheimer, G. Sastre, D. Volkmer, *Adv. Funct. Mater.* **2014**, *24*, 3885–3896.

[4] A. B. Cairns, A. L. Goodwin, *Chem. Soc. Rev.* **2013**, *42*, 4881–4893.

[5] a) E. Pardo, C. Train, H. Liu, L. M. Chamoreau, B. Dkhil, K. Boubekeur, F. Lloret, K. Nakatani, H. Tokoro, S. i. Ohkoshi, M. Verdaguer, *Angew. Chem. Int. Ed.* **2012**, *51*, 8356–8360; *Angew.*

Chem. **2012**, *124*, 8481 – 8485; b) S. i. Ohkoshi, H. Tokoro, T. Matsuda, H. Takahashi, H. Irie, K. Hashimoto, *Angew. Chem. Int. Ed.* **2007**, *46*, 3238 – 3241; *Angew. Chem.* **2007**, *119*, 3302 – 3305; c) H. B. Cui, Z. M. Wang, K. Takahashi, Y. Okano, H. Kobayashi, A. Kobayashi, *J. Am. Chem. Soc.* **2006**, *128*, 15074 – 15075.

[6] a) R. Shang, S. Chen, Z. M. Wang, S. Gao in *Metal-Organic Framework Materials* (Eds.: L. R. Macgillivray, C. M. Lukehart), John Wiley & Sons, Ltd: Chichester, UK, **2014,** DOI: 10.1002/9781119951438.eibc2215; b) Z. M. Wang, K. L. Hu, S. Gao, H. Kobayashi, *Adv. Mater.* **2010**, *22*, 1526 – 1533.

[7] a) E. C. Spencer, M. S. R. N. Kiran, W. Li, U. Ramamurty, N. L. Ross, A. K. Cheetham, *Angew. Chem. Int. Ed.* **2014**, *53*, 5583 – 5586; *Angew. Chem.* **2014**, *126*, 5689 – 5692; b) W. Li, A. Thirumurugan, P. T. Barton, Z. Lin, S. Henke, H. H.-M. Yeung, M. T. Wharmby, E. G. Bithell, C. J. Howard, A. K. Cheetham, *J. Am. Chem. Soc.* **2014**, *136*, 7801 – 7804; c) W. Li, M. R. Probert, M. Kosa, T. D. Bennett, A. Thirumurugan, R. P. Burwood, M. Parinello, J. A. K. Howard, A. K. Cheetham, *J. Am. Chem. Soc.* **2012**, *134*, 11940 – 11943.

[8] B. Zhou, Y. Imai, A. Kobayashi, Z.-M. Wang, H. Kobayashi, *Angew. Chem. Int. Ed.* **2011**, *50*, 11441 – 11445; *Angew. Chem.* **2011**, *123*, 11643 – 11647.

[9] a) D.-W. Fu, W. Zhang, H.-L. Cai, Y. Zhang, J.-Z. Ge, R.-G. Xiong, S. D. Huang, T. Nakamura, *Angew. Chem. Int. Ed.* **2011**, *50*, 11947 – 11951; *Angew. Chem.* **2011**, *123*, 12153 – 12157; b) P. Jain, V. Ramachandran, R. J. Clark, H. D. Zhou, B. H. Toby, N. S. Dalal, H. W. Kroto, A. K. Cheetham, *J. Am. Chem. Soc.* **2009**, *131*, 13625 – 13627; c) M. Sánchez-Andújar, S. Presedo, S. Yáñez-Vilar, S. Castro-García, J. Shamir, M. A. Señarís-Rodríguez, *Inorg. Chem.* **2010**, *49*, 1510 – 1516.

[10] a) G.-C. Xu, W. Zhang, X.-M. Ma, Y.-H. Chen, L. Zhang, H.-L. Cai, Z.-M. Wang, R.-G. Xiong, S. Gao, *J. Am. Chem. Soc.* **2011**, *133*, 14948 – 14951; b) G.-C. Xu, X.-M. Ma, L. Zhang, Z.-M. Wang, S. Gao, *J. Am. Chem. Soc.* **2010**, *132*, 9588 – 9590.

[11] a) R. Shang, S. Chen, K. L. Hu, Z. C. Jiang, B. W. Wang, M. Kurmoo, Z. M. Wang, S. Gao, *APL Mater.* **2014**, *2*, 124104; b) R. Shang, S. Chen, Z. M. Wang, S. Gao, *Chem. Eur. J.* **2014**, *20*, 15872 – 15883; c) R. Shang, G. C. Xu, Z. M. Wang, S. Gao, *Chem. Eur. J.* **2014**, *20*, 1146 – 1158; d) S. Chen, R. Shang, K. L. Hu, Z. M. Wang, S. Gao, *Inorg. Chem. Front.* **2014**, *1*, 83 – 98.

[12] L. Cañadillas-Delgado, O. Fabelo, J. A. Rodríguez-Velamazán, M. Lemée-Cailleau, S. A. Mason, E. Pardo, F. Lloret, J. Zhao, X. Bu, V. Simonet, C. V. Colin, J. Rodríguez-Carvajal, *J. Am. Chem. Soc.* **2012**, *134*, 19772 – 19781.

[13] a) M. Y. Li, B. Liu, B. W. Wang, Z. M. Wang, S. Gao, M. Kurmoo, *Dalton Trans.* **2011**, *40*, 6038 – 6046; b) M.-Y. Li, M. Kurmoo, Z. M. Wang, S. Gao, *Chem. Asian J.* **2011**, *6*, 3084 – 3096.

[14] a) M. E. Lines, A. M. Glass, *Principles and Applications of Ferroelectrics and Related Materials*, Clarendon Press, Oxford, **1977**; b) W. Känzig, *Ferroelectrics and Antiferroelectrics*, Academic Press, New York and London, **1957**.

[15] S. R. Batten, R. Robson, *Angew. Chem. Int. Ed.* **1998**, *37*, 1460 – 1494; *Angew. Chem.* **1998**, *110*, 1558 – 1595.

[16] a) A. K. Jonscher, *Dielectric Relaxation in Solids*, Chelsea Dielectrics Press, London, **1983**; b) G. G. Raju, *Dielectrics in Electric Fields*, Marcel Dekker, New York, **2003**.

